

Hydrothermal Synthesis, Characterization, and Thermodynamic Properties of a New Lithium Borate, $\text{Li}_3\text{B}_5\text{O}_8(\text{OH})_2$

Ping Li and Zhi-Hong Liu*

Key Laboratory for Macromolecular Science of Shaanxi Province, School of Chemistry and Materials Science, Shaanxi Normal University, Xi'an 710062, People's Republic of China

A new lithium borate $\text{Li}_3\text{B}_5\text{O}_8(\text{OH})_2$ (**I**), which is the enantiomer of the known $\text{Li}_3\text{B}_5\text{O}_8(\text{OH})_2$ (**II**), has been synthesized under mild hydrothermal conditions. Its crystal structure was determined from single crystal X-ray diffraction (XRD) data, further characterized by Fourier transform infrared (FT-IR) spectroscopy, Raman spectroscopy, XRD, differential thermal/thermogravimetric analysis (DTA-TG), and chemical analysis. It belongs to the tetragonal system, space group $P4_32_12$, with $a = 6.8506(9)$ Å, $c = 14.5601(15)$ Å, $V = 683.32(15)$ Å³, and $Z = 4$. Through an appropriate thermochemical cycle, the standard molar enthalpy of formation of $\text{Li}_3\text{B}_5\text{O}_8(\text{OH})_2$ was determined to be $-(4724.1 \pm 4.2)$ kJ·mol⁻¹ by solution calorimetry. Comparison of the experimental results with that of its enantiomer shows that the pair of enantiomers have the same standard molar enthalpy of formation like many other properties.

Introduction

Boron can form a large variety of compounds because of the complexity of the structures involved. In the past several decades, much interest has focused on studies of alkali metal borates because some of these compounds show interesting physical properties, such as nonlinear optical behavior for LiB_3O_5 (LBO), $\text{CsLiB}_6\text{O}_{10}$ (CLBO), and $\text{KB}_5\text{O}_8 \cdot 4\text{H}_2\text{O}$.^{1,2} So far, several phases have been obtained in the $\text{Li}_2\text{O}-\text{B}_2\text{O}_3-\text{H}_2\text{O}$ system, such as $\text{Li}(\text{H}_2\text{O})_4\text{B}(\text{OH})_4 \cdot 2\text{H}_2\text{O}$,³ $\text{LiB}(\text{OH})_4$,⁴ $\text{LiB}_5\text{O}_7(\text{OH})_2$,⁵ $\text{LiB}_2\text{O}_3(\text{OH}) \cdot \text{H}_2\text{O}$,⁶ $\text{Li}_3\text{B}_5\text{O}_8(\text{OH})_2$,^{7,8} and $\text{Li}_8[\text{B}_{16}\text{O}_{26}(\text{OH})_4] \cdot 6\text{H}_2\text{O}$.⁹ Of these, $\text{Li}_3\text{B}_5\text{O}_8(\text{OH})_2$ can be used for fast ionic conductivity.¹⁰ Recently, we obtained a new lithium borate of $\text{Li}_3\text{B}_5\text{O}_8(\text{OH})_2$ (**I**), which is the enantiomer of the known $\text{Li}_3\text{B}_5\text{O}_8(\text{OH})_2$ (**II**).^{7,8} In this paper, we describe the synthesis, characterization, and the determination of the standard molar enthalpy of formation of $\text{Li}_3\text{B}_5\text{O}_8(\text{OH})_2$ (**I**) by using a heat conduction microcalorimeter, as part of the continuing study of the thermochemistry of hydrated lithium borates.^{11–13} As a comparison, we also determined the standard molar enthalpy of formation of $\text{Li}_3\text{B}_5\text{O}_8(\text{OH})_2$ (**II**).

Experimental Section

Synthesis and Characterization of Samples. All reagents used in the synthesis of **I** and **II** were of analytical grade. For **I**, a mixture of 0.738 g of Li_2CO_3 , 3.092 g of H_3BO_3 , 0.325 g of La_2O_3 , 7.0 cm³ of pyridine, and 4.0 cm³ of H_2O was sealed in a Teflon lined bomb, heated at 180 °C for 7 days, and then cooled to room temperature. For **II**, a mixture of 0.618 g of H_3BO_3 , 2.233 g of $\text{Li}_2\text{B}_4\text{O}_7 \cdot 3\text{H}_2\text{O}$, 5.0 cm³ of pyridine, and 1.0 cm³ of H_2O was sealed in a Teflon lined bomb, heated at 170 °C for 3 days, and then cooled to room temperature. The resulting products were recovered by filtration, washed with distilled water, and dried in a vacuum dryer to a constant mass at room temperature. The samples of **I** and **II** were characterized by Fourier transform infrared (FT-IR) spectroscopy (recorded

Table 1. Crystal Data and Structure Refinement for I

empirical formula	$\text{H}_2\text{B}_5\text{Li}_3\text{O}_{10}$
formula weight	236.89
crystal system, space group	tetragonal, $P4_32_12$
unit cell dimensions	$a = 6.8506(9)$ Å, $\alpha = 90^\circ$ $b = 6.8506(9)$ Å, $\beta = 90^\circ$ $c = 14.5601(15)$ Å, $\gamma = 90^\circ$
volume	$683.32(15)$ Å ³
Z, calculated density	4, 2.303 g·cm ⁻³
crystal size	$0.53 \times 0.49 \times 0.48$ mm ³
temperature	298(2) K
wavelength	0.71073 Å
absorption coefficient	0.214 mm ⁻¹
$F(000)$	464
θ range for data collection	(3.29 to 25.01)°
limiting indices	$-7 \leq h \leq 8$, $-4 \leq k \leq 8$, $-17 \leq l \leq 16$
reflections collected/unique	3487/630 [$R(\text{int}) = 0.0204$]
absorption correction	semiempirical from equivalents
max. and min. transmission	0.9041 and 0.8949
refinement method	full-matrix least-squares on F^2
goodness-of-fit on F^2	1.024
final R indices [$I > 2\sigma(I)$]	$R_1 = 0.0210$, $wR_2 = 0.0572$
R indices (all data)	$R_1 = 0.0215$, $wR_2 = 0.0576$
largest diff. peak and hole	(0.139 and -0.153) e·Å ⁻³

over the (400 to 4000) cm⁻¹ region on a Bruker Equinox 55 spectrometer with KBr pellets at room temperature), Raman spectroscopy (recorded over the (300 to 4000) cm⁻¹ region on a Nicolet Almega dispersive Raman spectrometer), X-ray powder diffraction (Rigaku D/MAX-IIIIC with Cu target at 8 deg·min⁻¹), thermogravimetric analysis (TGA), and differential thermal analysis (DTA) (performed on a SDT Q600 simultaneous thermal analyzer under N_2 atmosphere with a heating rate of 10 °C·min⁻¹). The B_2O_3 content was determined by NaOH titration in the presence of mannitol.

Determination of Crystal Structure. A colorless, transparent crystal (**I**) of $0.53 \times 0.49 \times 0.48$ mm³ size was selected for the crystal structure measurement. The X-ray diffraction intensities were recorded by a Bruker Smart-1000 charge-coupled device (CCD) diffractometer with graphite monochromatized Mo $K\alpha$ radiation ($\lambda = 0.071073$ nm). Crystal data and conditions of the intensity measurements are given in Table 1 (CSD-418166).

* Corresponding author. Tel.: +86 29 8530 7765; fax: +86 29 8530 7774. E-mail address: liuzh@snnu.edu.cn.

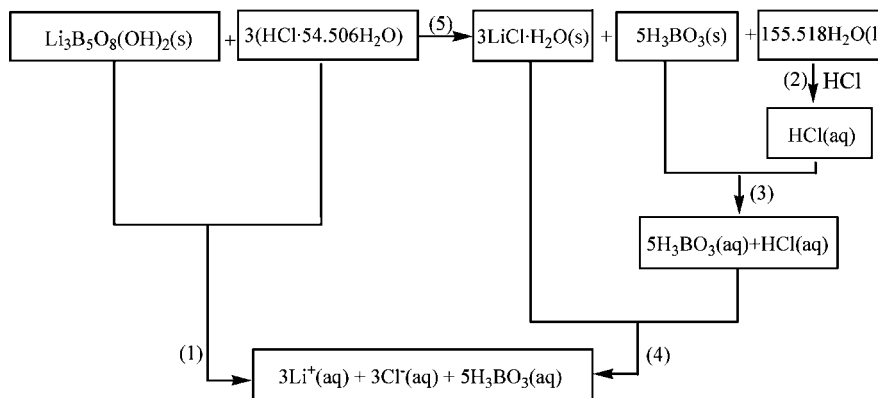


Figure 1. Designed thermochemical cycle.

Method of the Calorimetric Experiment. The thermochemical cycle designed for the derivation of the $\Delta_f H_m^\circ$ of $\text{Li}_3\text{B}_5\text{O}_8(\text{OH})_2$ is shown in Figure 1. The $1 \text{ mol} \cdot \text{dm}^{-3}$ $\text{HCl}(\text{aq})$ solvent can dissolve instantaneously all components of reaction 5. In all of these determinations, a strict control of the stoichiometries in each step of the calorimetric cycle must be obeyed, with the objective that the dissolution of the reactants gives the same composition as those of the products. Applying Hess' law, $\Delta_f H_m^\circ(5)$ could be calculated according to the following expression:

$$\Delta_f H_m^\circ(5) = \Delta_f H_m^\circ(1) - \Delta_f H_m^\circ(2) - \Delta_f H_m^\circ(3) - \Delta_f H_m^\circ(4)$$

The standard molar enthalpy of formation of $\text{Li}_3\text{B}_5\text{O}_8(\text{OH})_2$ could be obtained by the value of $\Delta_f H_m^\circ(5)$ in combination with the standard molar enthalpies of formation of $\text{LiCl} \cdot \text{H}_2\text{O}(\text{s})$, $\text{H}_3\text{BO}_3(\text{s})$, $\text{HCl}(\text{aq})$, and $\text{H}_2\text{O}(\text{l})$.

The RD496-III heat conduction calorimeter (Southwest Institute of Electron Engineering, China) used was described in detail previously.^{14,15} To check the performance of the calorimeter, the enthalpy of solution of KCl (mass fraction ≥ 0.9999) in deionized water was determined to be $(17.31 \pm 0.20) \text{ kJ} \cdot \text{mol}^{-1}$, which is in agreement with that of $17.234 \text{ kJ} \cdot \text{mol}^{-1}$ reported in the literature.¹⁶ This shows that the device used for measuring the enthalpy of solution in this work is reliable. Calorimetric experiments were performed five times at 298.15 K as previously described.¹⁵ No solid residues were observed after the reactions.

Results and Discussion

Description of the Crystal Structure of $\text{Li}_3\text{B}_5\text{O}_8(\text{OH})_2$ (I).

The crystal was found to be tetragonal, with space group $P4_32_12$, with $a = 6.8506(9) \text{ \AA}$, $c = 14.5601(15) \text{ \AA}$, $V = 683.32(15) \text{ \AA}^3$, and $Z = 4$. The main bond lengths and angles are listed in Table 2. The crystal structure of $\text{Li}_3\text{B}_5\text{O}_8(\text{OH})_2$ consists of $\text{Li}-\text{O}$ polyhedra and the $[\text{B}_5\text{O}_8(\text{OH})_2]^{3-}$ polyborate anion (Figure 2). The $[\text{B}_5\text{O}_8(\text{OH})_2]^{3-}$ polyborate anion consists of two six-membered rings in which two boron atoms (B1A and B1B) are surrounded by three oxygen atoms, and the other three boron atoms (B2, B2A, and B3) are surrounded by four oxygen atoms. Each six-membered ring is linked by a common BO_3 tetrahedron and consists of one BO_3 triangle (Δ), one $\text{BO}_3(\text{OH})$ tetrahedron (T), and a common BO_4 tetrahedron. The mean B–O distances of the BO_3 and BO_4 groups are $(1.383$ and $1.492) \text{ \AA}$, respectively (Table 2). The $[\text{B}_5\text{O}_8(\text{OH})_2]^{3-}$ units are linked together through four exocyclic oxygen atoms (O4, O4A, O4B, and O4C) to neighboring units and formed a three-dimensional structure, as shown in Figure 3. Moreover, there also exist hydrogen bonds

Table 2. Main Bond Lengths (\AA) and Angles (deg) of I^a

Li(1)–O(5)#1	1.962(3)	Li(2)–O(2)#8	2.056(3)
Li(1)–O(3)#2	2.009(3)	Li(2)–O(4)#6	2.436(3)
Li(1)–O(2)	2.035(3)	Li(2)–O(4)	2.436(3)
Li(1)–O(5)#3	2.112(3)	B(1)–O(3)#2	1.3765(18)
Li(1)–O(3)	2.403(3)	B(2)–O(1)#11	1.4772(18)
Li(2)–O(1)#6	2.0242(15)	B(3)–O(2)#12	1.4636(15)
Li(2)–O(1)	2.0242(15)	B(3)–O(3)#12	1.4964(16)
Li(2)–O(2)#7	2.056(3)		
B(1)#3–O(3)–B(3)	121.46(11)	O(5)–B(2)–O(4)	108.45(11)
B(1)–O(4)–B(2)	124.14(12)	O(1)#11–B(2)–O(4)	105.64(11)
O(1)–B(1)–O(4)	117.19(13)	O(2)#12–B(3)–O(2)	109.86(16)
O(1)–B(1)–O(3)#2	121.98(13)	O(2)#12–B(3)–O(3)	111.12(5)
O(4)–B(1)–O(3)#2	120.83(14)	O(2)–B(3)–O(3)	107.69(5)
O(2)–B(2)–O(5)	110.03(12)	O(2)#12–B(3)–O(3)#12	107.69(5)
O(2)–B(2)–O(1)#11	110.89(11)	O(2)–B(3)–O(3)#12	111.12(5)
O(5)–B(2)–O(1)#11	109.89(11)	O(3)–B(3)–O(3)#12	109.39(16)
O(2)–B(2)–O(4)	111.81(11)		

^a Symmetry transformations used to generate equivalent atoms: #2, $x - 1/2, -y + 1/2, -z + 1/4$; #3, $x + 1/2, -y + 1/2, -z + 1/4$; #11, $-y + 3/2, x - 1/2, z - 1/4$; #12, $y + 1, x - 1, -z$.

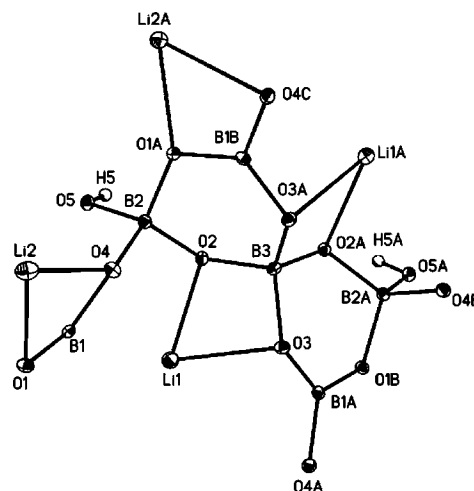


Figure 2. Asymmetric unit structure of I.

between the framework hydroxyl groups and the exocyclic oxygen atoms, $\text{O5}-\text{H5} \cdots \text{O4}$ ($y, x - 1, -z$). The H-bonded $\text{O} \cdots \text{O}$ distance is 2.987 \AA . According to the classification of polyborate anions proposed by Heller¹⁷ and Christ and Clark,¹⁸ the shorthand notation for $[\text{B}_5\text{O}_8(\text{OH})_2]^{3-}$ in $\text{Li}_3\text{B}_5\text{O}_8(\text{OH})_2$ is $5:_{\infty}^3[5: 2\Delta + 3\text{T}]$.

All of the Li^+ ions are located in the anionic $[\text{B}_5\text{O}_8(\text{OH})_2]^{3-}$ framework and compensate its negative charge. There are two kinds of coordinated forms for Li^+ ions (Figure 2 and Figure S1 in Supporting Information). Li1 exhibits a five-fold coordination and coordinates to three oxygen atoms (O2, O3, and O3B) from B–O–B bridges and two oxygen atoms (O5B and O5C)

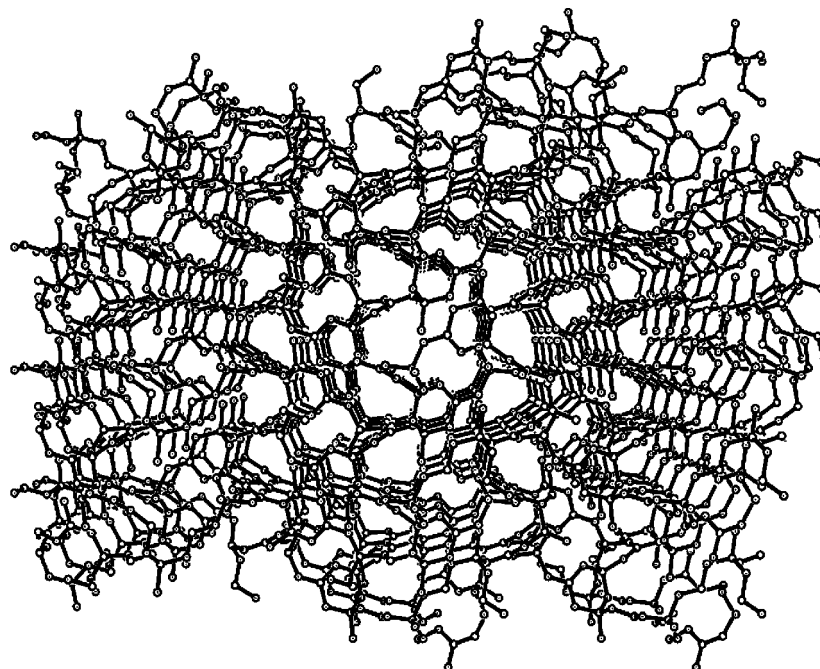


Figure 3. View of the three-dimensional framework along the a axis in **I**.

from hydroxyl groups, in which the Li–O distances range from (1.962 to 2.403) Å with a mean value of 2.1042 Å. Li2 exhibits a six-fold coordination and coordinates to four oxygen atoms (O1, O1C, O2B, and O2C) from B–O–B bridges and two exocyclic oxygen atoms (O4 and O4D), in which the Li–O distances range from (2.024 to 2.436) Å with a mean value of 2.172 Å.

The known $\text{Li}_3\text{B}_5\text{O}_8(\text{OH})_2$ (**II**)^{7,8} belongs to a tetragonal system, with space group $P4_12_12$, with $a = 6.8455(4)$ Å, $c = 14.551(1)$ Å, and $Z = 4$. Comparing the crystal data of the present borate with those of the known $\text{Li}_3\text{B}_5\text{O}_8(\text{OH})_2$, it can be thought that the present borate is a new compound, which is an enantiomer of the known $\text{Li}_3\text{B}_5\text{O}_8(\text{OH})_2$. It is the different synthesis conditions that might result in the two different forms; the starting materials for known $\text{Li}_3\text{B}_5\text{O}_8(\text{OH})_2$ (**II**) are $\text{LiOH}\cdot\text{H}_2\text{O}$, H_3BO_3 , and H_2O , but the starting materials for the present $\text{Li}_3\text{B}_5\text{O}_8(\text{OH})_2$ (**I**) are Li_2CO_3 , H_3BO_3 , La_2O_3 , pyridine, and H_2O .

Characterization of the Synthetic Samples. The chemical analytical data of the synthetic samples are (found/calcd, %), B_2O_3 (73.22/73.47) for **I**, and B_2O_3 (73.52/73.47) for **II**, which are consistent with the theoretical values.

The powder XRD pattern of the as-synthesized compound (**I**) and the simulated pattern on the basis of single-crystal structure of $\text{Li}_3\text{B}_5\text{O}_8(\text{OH})_2$ are shown in Figure 4. The diffraction peaks on patterns corresponded well in position, indicating the phase purity of the as-synthesized sample (**I**). The main characteristic d values and 2θ of the XRD pattern for (**II**) are given in Table S1 in the Supporting Information, which correspond with those of the JCPDS card (File No. 44-0249) and show the absence of any other crystalline forms in this synthetic sample.

The FT-IR (Figure S2, Supporting Information) and Raman (Figure S3, Supporting Information) spectra of **I** and **II** exhibited the following absorption bands and Raman shifts, which were assigned referring to the literature.¹⁹ IR: The band at 3439 cm^{-1} is the stretching of O–H. The bands at (1334 and 943 cm^{-1}) might be the asymmetric and symmetric stretching of $\text{B}_{(3)}\text{--O}$, respectively. The band at 1231 cm^{-1} might be the in-plane

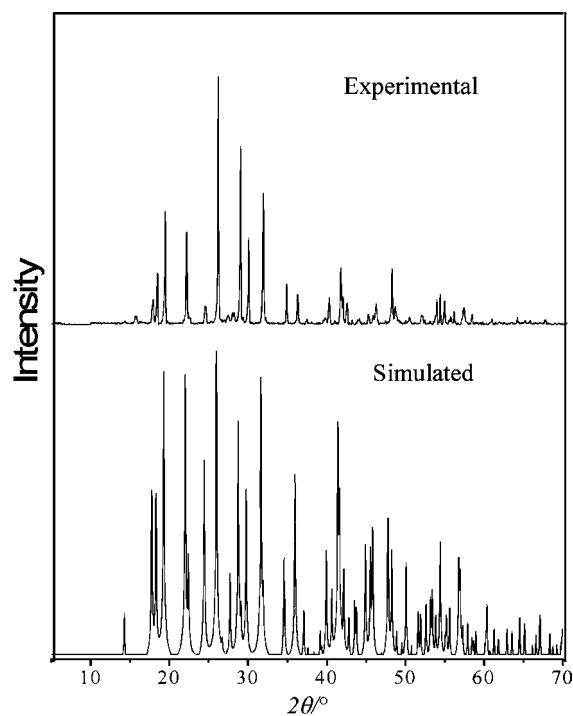


Figure 4. Powder XRD pattern of the sample **I**.

bending of B–O–H. The bands at (1112, 998, and 871 cm^{-1}) are the asymmetric and symmetric stretching of $\text{B}_{(4)}\text{--O}$, respectively. The bands at (723 and 650 cm^{-1}) are assigned as the out-of-plane bending of $\text{B}_{(3)}\text{--O}$. The bands at (526 and 460 cm^{-1}) are the bending of $\text{B}_{(3)}\text{--O}$ and $\text{B}_{(4)}\text{--O}$, respectively. Raman: The peak at 3436 cm^{-1} is the stretching of O–H. The peaks at (841 and 757 cm^{-1}) are the symmetric stretching of $\text{B}_{(4)}\text{--O}$. The peaks at (580 and 547 cm^{-1}) might be the bending of $\text{B}_{(3)}\text{--O}$ and $\text{B}_{(4)}\text{--O}$.

The simultaneous TG-DTA curves of **I** (Figure 5) and **II** (Figure S4, Supporting Information) indicate that both compounds are stable up to about $450\text{ }^\circ\text{C}$ and then have one step of mass loss between (450 and $600\text{ }^\circ\text{C}$). The total mass loss is

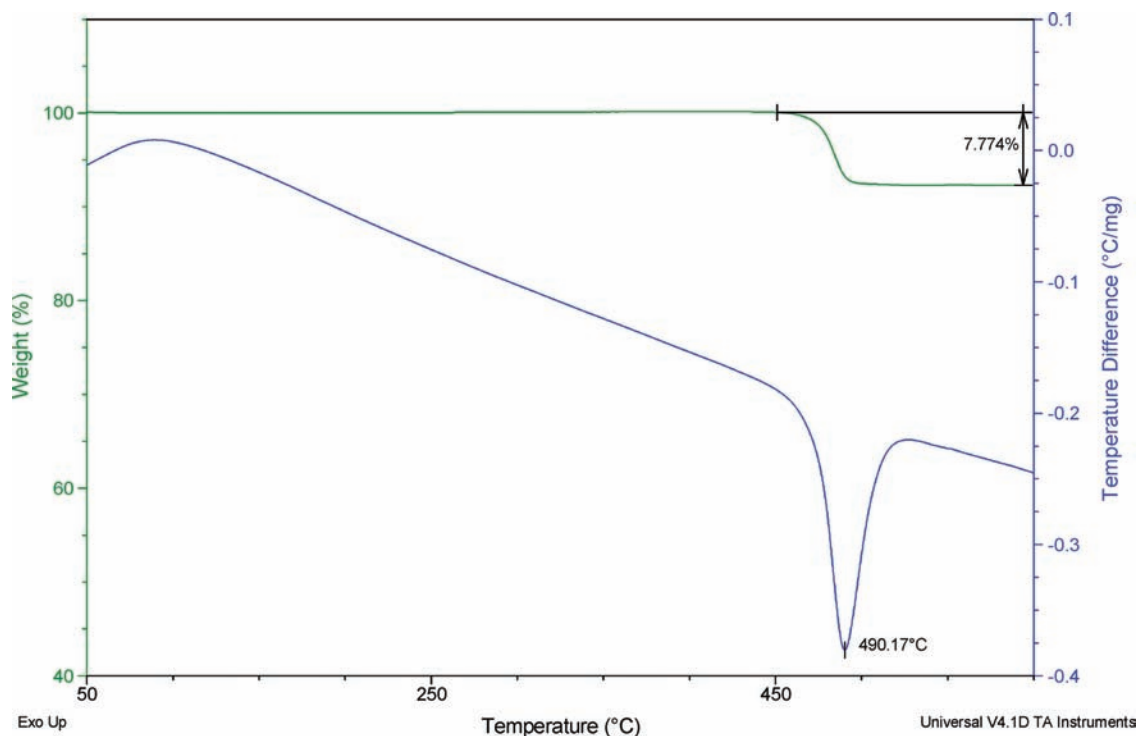


Figure 5. Simultaneous TG-DTA curves of the sample I.

Table 3. Molar Enthalpies of Solution of $\text{Li}_3\text{B}_5\text{O}_8(\text{OH})_2$ in $1 \text{ mol} \cdot \text{dm}^{-3} \text{ HCl}(\text{aq})$ at 298.15 K^a

no.	m mg	$\Delta_r H$ mJ	$\Delta_{\text{sol}} H_m$ $\text{kJ} \cdot \text{mol}^{-1}$
I			
1	9.49	-1662.646	-41.502
2	9.56	-1666.133	-41.285
3	9.40	-1659.450	-41.819
4	9.45	-1668.561	-41.826
5	9.42	-1650.323	-41.501
mean			-41.57 ± 0.21^b
II			
1	5.48	-981.773	-42.439
2	5.52	-969.406	-41.601
3	5.55	-971.667	-41.472
4	5.29	-928.550	-41.580
5	5.54	-984.236	-42.085
mean			-41.84 ± 0.37^b

^a In each experiment, 2.00 cm^3 of $\text{HCl}(\text{aq})$ was used. ^b Uncertainty is estimated as twice the standard deviation of the mean, namely, $\delta = 2[\sum(x_i - \bar{x})^2/n(n-1)]^{1/2}$, in which n is the number of experimentals ($n = 5$), x_i is the experimental value of each repeated measurement, and \bar{x} is the mean value.

Table 4. Thermochemical Cycle and Results for the Derivation of $\Delta_r H_m^\circ(\text{Li}_3\text{B}_5\text{O}_8(\text{OH})_2, 298.15 \text{ K})$

no.	reaction	$\Delta_r H_m^\circ$ $\text{kJ} \cdot \text{mol}^{-1}$
(1)	$\text{Li}_3\text{B}_5\text{O}_8(\text{OH})_2(\text{s}) + 50.04(\text{HCl} \cdot 54.506\text{H}_2\text{O}) = 3\text{Li}^+(\text{aq}) + 3\text{Cl}^-(\text{aq}) + 5\text{H}_3\text{BO}_3(\text{aq}) + 47.04(\text{HCl} \cdot 57.876\text{H}_2\text{O})$	-41.57 ± 0.21 (I)
(2)	$47.04(\text{HCl} \cdot 57.876\text{H}_2\text{O}) = 47.04(\text{HCl} \cdot 54.506\text{H}_2\text{O}) + 158.518\text{H}_2\text{O}(\text{l})$	-41.84 ± 0.37 (II)
(3)	$5\text{H}_3\text{BO}_3(\text{aq}) + 47.04(\text{HCl} \cdot 57.876\text{H}_2\text{O}) = 5\text{H}_3\text{BO}_3(\text{s}) + 47.04(\text{HCl} \cdot 57.876\text{H}_2\text{O})$	3.02 ± 0.12
(4)	$3\text{Li}^+(\text{aq}) + 3\text{Cl}^-(\text{aq}) + 5\text{H}_3\text{BO}_3(\text{aq}) + 47.04(\text{HCl} \cdot 57.876\text{H}_2\text{O}) = 3\text{LiCl} \cdot \text{H}_2\text{O}(\text{s}) + 5\text{H}_3\text{BO}_3(\text{aq}) + 47.04(\text{HCl} \cdot 57.876\text{H}_2\text{O})$	-109.15 ± 0.40
(5)	$3/2\text{H}_2(\text{g}) + 3/2\text{Cl}_2(\text{g}) + 163.518\text{H}_2\text{O}(\text{l}) = 3(\text{HCl} \cdot 54.506\text{H}_2\text{O})$	43.08 ± 0.11
(6)	$3\text{LiCl} \cdot \text{H}_2\text{O}(\text{s}) = 3\text{Li}(\text{s}) + 3/2\text{Cl}_2(\text{g}) + 3\text{H}_2(\text{g}) + 3/2\text{O}_2(\text{g})$	-496.37 ± 0.30
(7)	$5\text{H}_3\text{BO}_3(\text{s}) = 5\text{B}(\text{s}) + (15/2)\text{H}_2(\text{g}) + (15/2)\text{O}_2(\text{g})$	2137.74 ± 1.08
(8)	$8\text{H}_2(\text{g}) + 4\text{O}_2(\text{g}) = 8\text{H}_2\text{O}(\text{l})$	5474.00 ± 4.0
(9)	$\text{Li}_3\text{B}_5\text{O}_8(\text{OH})_2(\text{s}) = 3\text{Li}(\text{s}) + 5\text{B}(\text{s}) + \text{H}_2(\text{g}) + 5\text{O}_2(\text{g})$	-2286.64 ± 0.32
		4724.1 ± 4.19^a (I)
		4723.8 ± 4.21^a (II)

^a The uncertainty of the combined reaction is estimated as the square root of the sum of the squares of uncertainty of each individual reaction.

7.77 % for **I** and 8.08 % for **II**, which might correspond to the loss of one water molecule and can be compared with a calculated value of 7.60 %. In the DTA curve, the endothermic peak appearing at 490°C for **I** and 489°C for **II** is related to the one-step dehydration.

All of above results indicate that the synthetic samples are pure and suitable for the calorimetric experiments.

Results of the Calorimetric Experiment. The molar enthalpies of solution of **I** and **II** in $1 \text{ mol} \cdot \text{dm}^{-3} \text{ HCl}(\text{aq})$ at 298.15 K are listed in Table 3, in which m is the mass of sample, $\Delta_{\text{sol}} H_m$ is the molar enthalpy of solution of solute, and the uncertainty is estimated as twice the standard deviation of the mean.

Table 4 gives the thermochemical cycles for the derivation of the standard molar enthalpies of formation of **I** and **II**, respectively. The molar enthalpy of solution of $\text{H}_3\text{BO}_3(\text{s})$ of $(21.83 \pm 0.08) \text{ kJ} \cdot \text{mol}^{-1}$ in $1 \text{ mol} \cdot \text{dm}^{-3} \text{ HCl}(\text{aq})$ was taken from the literature.²⁰ The molar enthalpy of solution of $\text{LiCl} \cdot \text{H}_2\text{O}(\text{s})$ of $-(14.36 \pm 0.11) \text{ kJ} \cdot \text{mol}^{-1}$ in $(1 \text{ mol} \cdot \text{dm}^{-3} \text{ HCl} + \text{H}_3\text{BO}_3)(\text{aq})$ was taken from the literature.¹¹ The standard

molar enthalpy of formation of HCl(aq) and the enthalpy of dilution of HCl(aq) were calculated from the NBS tables.²¹ The standard molar enthalpy of formation of LiCl·H₂O(s) of $-(712.58 \pm 0.36)$ kJ·mol⁻¹ was taken from the NBS tables,²¹ and the standard molar enthalpies of formation of H₃BO₃(s) and H₂O(l) were taken from the CODATA key values,²² namely, $[-(1094.8 \pm 0.8)$ and $-(285.830 \pm 0.040)]$ kJ·mol⁻¹. From these data, the standard molar enthalpies of formation of **I** and **II** were calculated to be $-(4724.1 \pm 4.2)$ kJ·mol⁻¹ and $-(4723.8 \pm 4.2)$ kJ·mol⁻¹, respectively.

Conclusions

A new lithium borate Li₃B₅O₈(OH)₂ has been synthesized under mild hydrothermal conditions, which is an enantiomer of the known Li₃B₅O₈(OH)₂. It has a three-dimensional network structure. Through an appropriate thermochemical cycle, the standard molar enthalpies of formation of Li₃B₅O₈(OH)₂ (**I**) and (**II**) have been obtained by solution calorimetry; the result of which shows that the pair of enantiomers has the same standard molar enthalpy of formation like many other properties.

Supporting Information Available:

Figures showing additional FT-IR and Raman spectroscopy results and TG-DTA curves and table containing XRD information. This material is available free of charge via the Internet at <http://pubs.acs.org>.

Literature Cited

- (1) Wu, Y. C.; Sasaki, T.; Yokotani, A.; Tang, H. G.; Chen, C. T. CsB₃O₅: A new nonlinear optical crystal. *Appl. Phys. Lett.* **1993**, *62*, 2614–2615.
- (2) Dewey, C. F.; Cook, W. R.; Hodgson, R. T.; Wynne, J. J. Frequency doubling in KB₃O₈·4H₂O and NH₄B₅O₈·4H₂O to 217.3 nm. *Appl. Phys. Lett.* **1975**, *26*, 714–716.
- (3) Touboul, M.; Bétourné, E.; Nowogrocki, G. Crystal structure and dehydration process Li(H₂O)₄B(OH)₄·2H₂O. *J. Solid State Chem.* **1995**, *115*, 549–553.
- (4) Höhne, E. Lokalisierung der H-Atome in der Kristallstruktur des LiB(OH)₄. *Z. Anorg. Allg. Chem.* **1966**, *342*, 188–194.
- (5) Cárdenas, A.; Solans, J.; Byrappa, K.; Shekar, K. V. K. Structure of lithium catena-poly[3, 4-dihydroxopentaborate-1:5-μ-oxo]. *Acta Crystallogr.* **1993**, *C49*, 645–647.
- (6) Louër, D.; Louër, M.; Touboul, M. Crystal structure determination of lithium diborate hydrate, LiB₂O₃(OH)·H₂O, from X-ray powder

diffraction data collected with a curved position-sensitive detector. *J. Appl. Crystallogr.* **1992**, *25*, 617–623.

- (7) Bondareva, O. S.; Egorov-Tismenko, Y. K.; Simonov, M. A.; Belov, N. V. Crystal structure of lithium borate Li₃B₅O₈(OH)₂. *Sov. Phys. Dokl.* **1978**, *23* (11), 806–808.
- (8) Touboul, M.; Bétourné, E. New X-ray powder diffraction date for trillithium octaoxodihydroxopentaborate Li₃B₅O₈(OH)₂. *Powder Diffr.* **1993**, *8*, 162–163.
- (9) Li, P.; Liu, Z. H.; Ng, S. W. Li₈[B₁₆O₂₆(OH)₄]·6H₂O: A novel lithium borate with a larger polyborate anion. *Inorg. Chem. Commun.* **2008**, *11*, 893–895.
- (10) Byrappa, K.; Shekar, K. V. K.; Gali, S. Synthesis and characterization of Li₃B₅O₈(OH)₂ crystals. *Cryst. Res. Technol.* **1992**, *27*, 767–772.
- (11) Li, J.; Li, B.; Gao, S. Y. Thermochemistry of hydrated lithium borates. *J. Chem. Thermodyn.* **1998**, *30*, 681–688.
- (12) Zhu, L. X.; Gao, S. Y.; Xia, S. P. Thermochemistry of hydrated lithium monoborates. *Thermochim. Acta* **2004**, *419*, 105–108.
- (13) Li, P.; Liu, Z. H. Standard molar enthalpies of formation for the two alkali metal borates of Li₈[B₁₆O₂₆(OH)₄]·6H₂O and Cs₂[B₇O₉(OH)₅]. *J. Chem. Eng. Data* **2009**, *54*, 830–832.
- (14) Ji, M.; Liu, M. Y.; Gao, S. L.; Shi, Q. Z. The enthalpy of solution in water of complexes of zinc with methionine. *Instrum. Sci. Technol.* **2001**, *29*, 53–57.
- (15) Liu, Z. H.; Li, P.; Zuo, C. F. Standard molar enthalpies of formation for the two hydrated calcium borates xCaO·5B₂O₃·yH₂O (x = 2 and 4, y = 5 and 7). *J. Chem. Eng. Data* **2006**, *51*, 272–275.
- (16) Weast, R. C. *CRC Handbook of Chemistry and Physics*, 70th ed.; CRC Press: Boca Raton, FL, 1989.
- (17) Heller, G. A survey of structural types of borates and polyborates. *Top. Curr. Chem.* **1986**, *131*, 39–98.
- (18) Christ, C. L.; Clark, J. R. A crystal-chemical classification of borate structures with emphasis on hydrated borates. *Phys. Chem. Miner.* **1977**, *2*, 59–87.
- (19) Li, J.; Xia, S. P.; Gao, S. Y. FT-IR and Raman spectroscopic study of hydrated borates. *Spectrochim. Acta* **1995**, *51A*, 519–532.
- (20) Li, J.; Gao, S. Y.; Xia, S. P.; Li, B.; Hu, R. Z. Thermochemistry of hydrated magnesium borates. *J. Chem. Thermodyn.* **1997**, *29*, 491–497.
- (21) Wagman, D. D.; Evans, W. H.; Parker, V. B.; Schumm, R. H.; Halow, I.; Bailey, S. M.; Chumey, K. L.; Nuttall, R. L. The NBS Tables of Chemical Thermodynamic Properties. *J. Phys. Chem. Ref. Data* **1982**, *11*, 2.
- (22) Cox, J. D.; Wagman, D. D.; Medvedev, V. A. *CODATA Key Values for Thermodynamics*; Hemisphere: New York, 1989.

Received for review November 4, 2009. Accepted January 12, 2010. Project supported by the National Natural Science Foundation of China (No. 20871078) and Innovation Funds of Graduate Programs of Shaanxi Normal University (No. 2009CXB002).

JE900947D